

# **ATLAS 13 TeV Data Analysis using Particle Flow**

Christian Kirfel

Bachelorarbeit in Physik

angefertigt im Physikalischen Institut

vorgelegt der

Mathematisch-Naturwissenschaftlichen Fakultät

der

Rheinischen Friedrich-Wilhelms-Universität

Bonn

November 2016

DRAFT

Ich versichere, dass ich diese Arbeit selbstständig verfasst und keine anderen als die angegebenen Quellen und Hilfsmittel benutzt sowie die Zitate kenntlich gemacht habe.

Bonn, .....

Datum

.....

Unterschrift

1. Gutachter: Prof. Dr. John Smith
2. Gutachterin: Prof. Dr. Anne Jones

# Acknowledgements

---

I would like to thank ...

You should probably use \chapter\* for acknowledgements at the beginning of a thesis and \chapter for the end.

DRAFT

DRAFT

# Contents

---

<b>1</b>	<b>Introduction</b>	<b>1</b>
<b>2</b>	<b>Theoretical and experimental basics</b>	<b>3</b>
2.1	The Standard Model of Particle Physics . . . . .	3
2.2	The LHC and ATLAS . . . . .	5
2.2.1	The LHC . . . . .	5
2.2.2	The ATLAS Detector . . . . .	6
2.2.3	Tracking detectors . . . . .	6
2.2.4	Calorimeter . . . . .	8
<b>3</b>	<b>Particle Flow Reconstruction</b>	<b>9</b>
3.1	The Particle Flow Algorithm . . . . .	9
3.1.1	Track selection . . . . .	10
3.1.2	Clustering . . . . .	10
3.1.3	Matching Track to Cluster . . . . .	10
3.1.4	Cell Subtraction . . . . .	10
3.1.5	Eflow Rec performance studies . . . . .	11
3.1.6	Recent updates in eflowrec . . . . .	12
<b>4</b>	<b>Analysis framework</b>	<b>15</b>
4.1	Jet cleaning . . . . .	15
4.2	The Good Run List . . . . .	15
4.3	Jet Calibration and Smearing . . . . .	15
4.4	The jet vertex tagger . . . . .	15
4.5	Trigger Tools . . . . .	18
4.6	Monte Carlo Re-weighting . . . . .	18
4.7	Data Re-weighting . . . . .	18
4.8	Muon Calibration and Selection . . . . .	18
4.9	Electron Calibration and Selection . . . . .	18
<b>5</b>	<b>Results</b>	<b>19</b>
5.1	The $Z \rightarrow \mu\mu$ decay . . . . .	19
5.2	Event Selection . . . . .	19
5.3	Results . . . . .	19
<b>A</b>	<b>Useful information</b>	<b>21</b>
<b>List of Figures</b>		<b>23</b>

DRAFT

# CHAPTER 1

---

## Introduction

---

The Particle Flow algorithm is a promising approach of data analysis and has already been approved before on CMS as well as on ATLAS 2015 data. The combination of tracker and calorimeter information allows to improve the resolution especially in lower energy regions and can therefore reduce the energy threshold for analysis. The aim of my thesis was to create an analysis framework allowing Particle Flow analysis on 2016 13 TeV data and to show the improvements the new algorithm can yield. The second chapter of this thesis gives a brief introduction to the Standard Model of particle physics, the approved model used to describe most particle interactions, decays and crosssections. Furthermore the chapter includes a description of the ATLAS detector and its components and in addition a more general explanation of the attributes of tracking detectors and calorimeters to explain why better results are expected from the combination of both.

In the third chapter I describe the Particle Flow algorithm in detail and also present a brief overview of the Run 1 results as well as of the changes that have been applied to the algorithm since its first application in ATLAS.

Chapter four then summarizes the actual analysis framework that has been developed during my thesis. I give an explanation of all the important tools used in the framework and conclude by listing the difficulties and obstacles that still have to be overcome to complete a comprehensive analysis framework for Particle Flow.

Finally in chapter five I present the results derived from data/Monte Carlo comparison for 2016 data on  $Z \rightarrow \mu\mu$  events.



# CHAPTER 2

---

## Theoretical and experimental basics

---

### 2.1 The Standard Model of Particle Physics

The Standard Model of particle physics summarizes the current knowledge of fundamental particles and their interactions. The model applies to scales of 1 fm and below. Gravity, being the fourth fundamental force is not included as it is negligible for most phenomena at this scale.

The current view is that all matter is made out of three kinds of elementary particle being leptons quarks and mediators. There are six leptons falling into three families according to their charge, electron number, muon number and tau number.

Similar to that there are six flavors of quarks separated by strangeness (S), charm (C), beauty (B), and truth (T). As the leptons the quarks fall into three generations. For both kinds of particles the mass rises with the generations and each generation comes as a doublet. The first particle of each lepton doublet is uncharged and referred to as a neutrino while the second particle has charge  $-1$ . For each quark doublet there is an element with fractional charge  $-\frac{1}{3}$  and an element with fractional charge  $\frac{2}{3}$ . To each of these particles exists an anti particle of opposite charge.

The third kind of particle included in the standard model is the mediator. Mediators are gauge bosons the exchange of which allows the particles to interact. There are four kinds of elementary interactions of which the strong electromagnetic and weak interaction are included in the model. The fourth interaction is the gravitational force. The gauge particles for the strong interaction are the gluons carrying colour charge, the electromagnetic mediator is the photon ( $\gamma$ ) and the weak mediators are the  $W^\pm$  and  $Z$  bosons. Tables 2.1, 2.2 and 2.3 summarize the particles and their important properties.

Table 2.1: Lepton properties

	symbol	Charge	$L_e$	$L_\mu$	$L_\tau$
First generation {	$e$	-1	1	0	0
	$\nu_e$	0	1	0	0
Second generation {	$\mu$	-1	0	1	0
	$\nu_\mu$	0	0	1	0
Third generation {	$\tau$	-1	0	0	1
	$\nu_\tau$	0	0	0	1

Table 2.2: Quark properties

	Symbol	Charge Q	mass	D	U	S	C	B	T
First generation {	$d$	$-\frac{1}{3}$	4.8 MeV	-1	0	0	0	0	0
	$u$	$\frac{2}{3}$	2.3 MeV	0	1	0	0	0	0
Second generation {	$s$	$-\frac{1}{3}$	95 MeV	0	0	-1	0	0	0
	$c$	$\frac{2}{3}$	1 275 MeV	0	0	0	1	0	0
Third generation {	$b$	$-\frac{1}{3}$	4 180 MeV	0	0	0	0	-1	0
	$t$	$\frac{2}{3}$	173 210 MeV	0	0	0	0	0	1

Table 2.3: Mediator properties

Interaction	Theory	Mediator	Charge	Coupling
Strong	QCD	gluons (8)	colour	1
Electromagnetic	QED	photon $\gamma$	electric charge	$10^{-1}$
Weak	GSW	$W^\pm, Z$	weak isospin	$20^{-6}$

Given this the standard model of particle physics has been a very successful model for a very long time and still holds for most cases. Nevertheless the model has some commonly known weaknesses and does not claim to be complete. For example the gravitational force is not included and in the standard model neutrinos are massless which would not allow the oscillations observed in neutrinos originating from the sun. For further information check [**griffith08**], [**thomson13**] and [**brock11**].

There should be a short sentence about the Higgs Boson but I am unsure what to write exactly ?

## 2.2 The LHC and ATLAS

The analysis for this thesis has been performed in the ATLAS collaboration. The ATLAS-Detector is one of the four main experiments at the LHC at Cern. Therefore this chapter provides a brief overview over the LHC and ATLAS focusing on the properties directly relevant for Particle Flow Analysis.

After a description of the ATLAS detector in general I will give some further information about the detector components directly relevant for the explanation of particle flow which are the tracking detector and the calorimeter. To make the advantages of particle flow understandable to the reader I will give a general description of these detectors and their properties irrespective of their detailed construction at ATLAS.

### 2.2.1 The LHC

The Large Hadron Collider ("LHC") is part of the facilities of the European Organization of Nuclear Research ("CERN") and was built to extend the frontiers of modern particle physics by delivering high luminosities and unprecedented high energies. The Collider is circular with a circumference of 26.659 km and is located 10 km underground close to Geneva.

The LHC is designed to collide bunches of up to  $10^{11}$  protons at a luminosity of  $10^{34} \text{ cm}^{-2} \text{ s}^{-1}$ . The beams are collided at four collision points representing the four main experiments at the LHC. Two of these are special-purpose detectors, namely LHCb and ALICE while the other two are general-purpose detectors. The general-purpose experiments are CMS and ATLAS. The analysis in this thesis was performed on ATLAS data. Figure 2.1 shows the LHC, the four detectors and its general location.

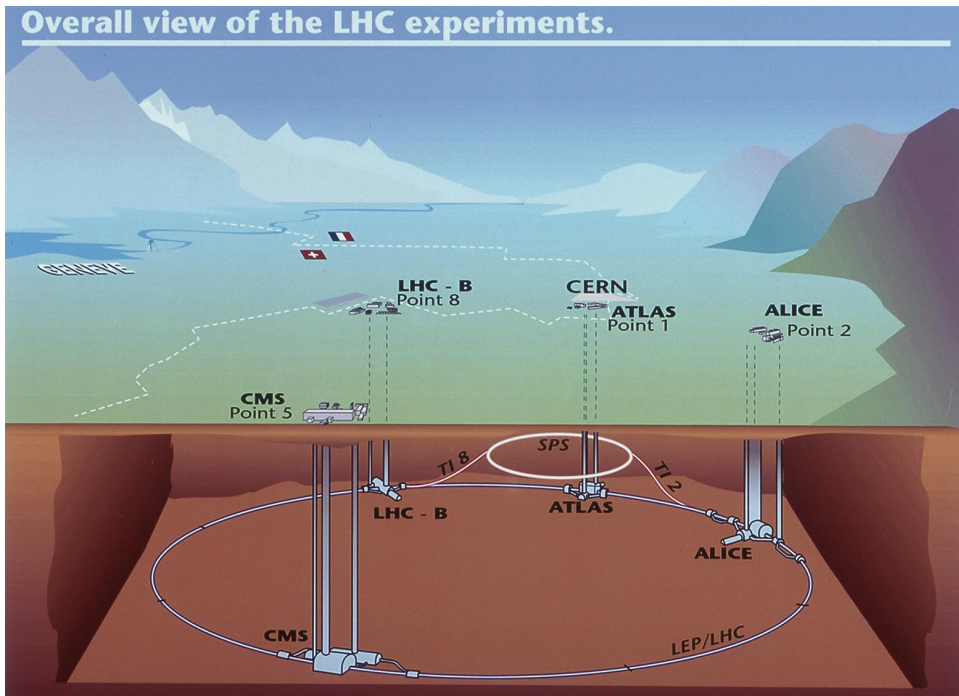


Figure 2.1: Sketch of the LHC ring, the position of the experiments and the surrounding countryside. The four big LHC experiments are indicated. The location of the injection lines and the SPS are also shown. [atlasfigures]

## 2.2.2 The ATLAS Detector

The ATLAS-Detector was developed to take advantage of the high energy available at the LHC enabling the observation of highly massive particles that lower energy accelerators were not able to create and that way bring new physics theory beyond the standard model of particle physics. It is designed to be able to observe a maximized number of final stages being a so called general purpose-detector. This means that the detector should be able to identify all kinds of particles and still provides an accurate information about angle and momentum. Figure 2.2 shows the outline of the ATLAS detector together with a rough scale in size. In the following explanations of its components are given from the inside to the outside.

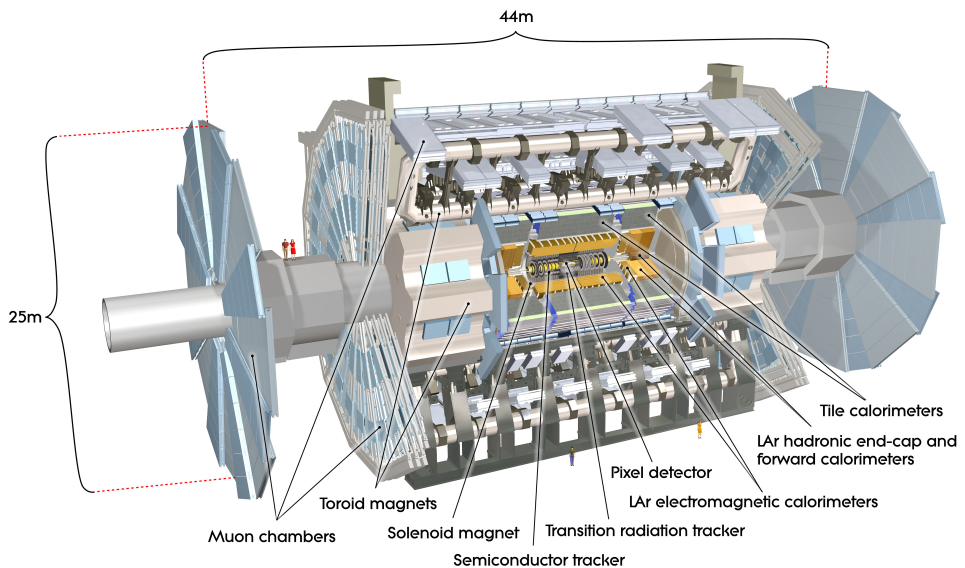


Figure 2.2: Sketch of the ATLAS detector [[atlasfigures](#)]

Figure 2.3 shows the detector's components in a simplified way and allows to understand the order of the important detector parts in detail. The innermost part of the detector is a tracking detector in a field of a large solenoid coil to obtain charge and trajectory of charged particles. The following two parts are the Electromagnetic and Hadronic Calorimeter which together build the Calorimeter part of the detector. One of them focuses on measuring the energy in electromagnetic showers while the other one is optimized for hadronic particle showers. The outermost part is a Muon spectrometer because most of the particles that cross the calorimeters undetected are muons.

## 2.2.3 Tracking detectors

The go to method to measure the momenta of charged particles is the usage of tracking detectors. These detectors are based on charged particles leaving a track of ionisations in any given medium and therefore by detecting this ionizations being able to reconstruct the particles trajectory. There are two main categories of tracking detectors in use. The first one uses a large gaseous volume in a strong electric field and is filled with a structure of wires. The electric field makes the liberating electrons drift towards the wires where they cause a detectable signal.

The second kind of detectors is based on semiconductor technology and is used in most modern detectors like ATLAS. Therefore I will describe this kind of tracking detectors in more detail. If a charged

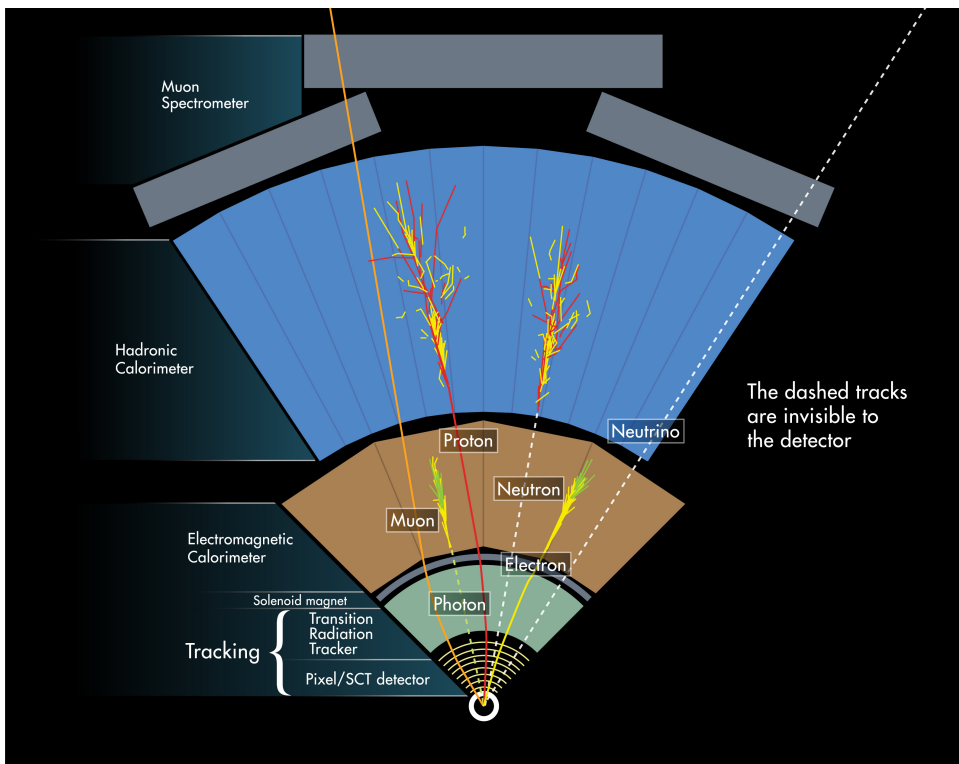


Figure 2.3: Scheme of the ATLAS-detector [atlasfigures]

particle traverses a appropriately doped semiconductor wafer for example a doped silicon wafer it creates electron hole pairs along its trail. If an electric field is applied to the semiconductor material the holes will drift in the direction of the electric field and can then be collected by p-n junctions.

Usually a tracking detector is divided into semiconductor strips or pixel with a magnitude of  $25\mu\text{m}$ . This way a signal at a certain junction can be used to reconstruct a trail and position. The common way to reconstruct a track is a set of cylindrical semiconductor wafers in a magnetic field. Each wafer signal gives a rough estimation of the particle's location at the time and the curve given by the sum of signals allows to calculate charge and momentum.

$$p \cdot \cos\lambda = 0.3BR \quad (2.1)$$

### Inner Detector

The Tracking detectors of the ATLAS detector are called the Inner Detector. It consists of three sub-components being the Pixel detector (Pixel), the Semi-Conductor Tracker (SCT) and a Transition Radiation Tracker (TRT). Each one of this sub-detectors is divided in a barrel part and two end-caps. The Inner detector covers a region of  $|\eta| < 2.5$  which also limits the region in which particle flow can be used.

### Muon spectrometer

The outermost part of the detector are the Muon tracking chambers or the so called muon spectrometer. The task of the spectrometer is to detect charged particles transversing the calorimeter undetected and to both trigger on them and to measure their energy. Due to these two functions the spectrometer is divided

into two parts each dedicated to one of the tasks. The first part is the trigger chamber covering a range of  $|\eta| < 2.4$  and with a range of  $|\eta| < 2.7$  comes the high-precision chamber as the second part. The main detectors support feet cause a further gap at about  $\phi = 300^\circ$  and  $\phi = 270^\circ$ .

The hih-precision detector uses Monitored Drift Tubes (MDTs) while the trigger chamber uses Resistive-Plate Chambers (RPCs). The momentum calculation then is performed by the field of the torroid magnet.

### 2.2.4 Calorimeter

In particle physics a calorimeter is a device to measure first and foremost the total energy of a particle. Most of the time also some positional information is taken. The idea is that most particles loose all their momentum crossing the calorimeter-structure. Measuring the energy deposited this way gives a measurement for the particle's energy. Usually a particle deposits its energy by initiating a particle shower. the shower's energy is then collected and measured. Calorimeters are distinguished by the main interaction of the particles one wants to detect.

#### Electromgnetic Calorimeter

Electromagnetic calorimeters are designed to detect charged particles and measure their total energy. Usually these particles are electrons and photons. There are various methods to construct these detectors. An example would be the usage of inorganic scintillators. These scintillators should be optically transparent and have a short radiation length to contain the shower in a compact region. The detection then can follow by photon detectors which measure the radiation light being proportional to the detected particle's energy. The energy resolution of these detectors is typically in the range

$$\frac{\sigma_E}{E} \sim \frac{3\% - 10\%}{\sqrt{E/GeV}}. \quad (2.2)$$

The electromagnetic calorimeter at ATLAS is a high-resolution and high-granularity liquid-argon sampling calorimeter. Leas is used as absorber material. The calorimeter consists of two half-barrels which are only divided by a small gap at the interaction point. The endcaps at each side are segmented into two coaxial wheels to cover different polar angles.

#### Hadronic calorimeters

Hadronic calorimeters are used to obtain the energies of hadronic particle showers. Due to the relatively large distance between interactions these calorimeters occupy a significantly large space in the detector.

A common technique to construct these calorimeters is a sandwich like structure of alternating layers of high density absorber material and active material. The absorbers are used to develop the particle showers which then hit the active material and deposit the energy there. That way hadronic calorimeters reach a resolution of about

$$\frac{\sigma_E}{E} \gtrsim \frac{50\%}{\sqrt{E/GeV}}. \quad (2.3)$$

For more information see the ATLAS design report [[atlastdr](#)]

# CHAPTER 3

---

## Particle Flow Reconstruction

---

One of the goals of this thesis was to check the results of Particle Flow in Run 2 data. Therefore this chapter will give an overview of the results that the new algorithm has brought for Run 1 in data MC comparison. Before showing the results this chapter gives a description of the algorithm based on the Particle Flow Paper [[pflow16](#)]. Then an update on how the algorithm has evolved is given before finally a brief overview of the results is presented.

### 3.1 The Particle Flow Algorithm

Recently only either the Calorimeter or the tracker information was used to reconstruct Jets in ATLAS events. The Particle Flow Algorithm combines tracker and calorimeter information to achieve better resolution especially at lower energies. The main advantages of including the tracker information into reconstruction are as follows:

- For low energy charged particles the momentum resolution of the tracking detector is superior to the calorimeter.
- The Tracking detector is able to reconstruct soft particles, which would not pass the noise threshold of the calorimeter.
- The ATLAS tracking detector has a superior angular resolution for single charged particles.
- Low  $p_T$  charged particles may be swept out of the cone before reaching the calorimeter by the magnetic field. The tracker information allows to cluster these particles into the jet.
- a better vertex determination could lower the pileup-contribution.

The advantages of Particle Flow have already been shown for Run 1 data in

Figure 3.1 sketches the important steps of the Particle Flow algorithm. The algorithm uses clusters from the calorimeters and tracks from the tracking detectors as input information. The first step is to match a track spatially to a cluster. After a pair has been found the algorithm checks whether the particle's momentum matches the energy deposited in the cluster within the expected deviation. If the energy matches a subtraction algorithm starts deciding which cells belong to the given event. If the energy deposited in the cluster is too low the algorithm includes all other clusters in a given area and then starts the subtraction.

After the subtraction the algorithm gives information about matched clusters and trackers. Furthermore energy deposited in cells that were not subtracted can be identified as remnants.

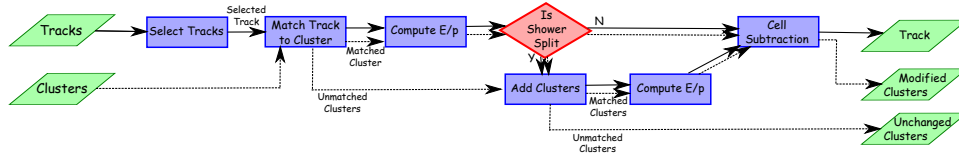


Figure 3.1: Flowchart of the steps of the Particle Flow algorithm [pflow16]

### 3.1.1 Track selection

In spite of the clusters the algorithm has some requirements on tracks to be selected to minimize the amount of fake tracks. The requirements are at least 9 hits in the PIXEL and SCT and no missing hits in the PIXEL at all. The tracks have to be in a pseudo-rapidity region of  $|\eta| < 2.5$  and  $500 \text{ MeV} < p_T < 40 \text{ GeV}$ .

### 3.1.2 Clustering

The algorithm uses information from the tracker and the calorimeter as input. The information from the calorimeter is give as topological clusters. The construction of these clusters is briefly described in this chapter to give the reader a basic understanding which input information the algorithm uses. Every cluster is being constructed around a so called seed cell. A seed cell is a cell for which the deposited energy exceeds the expected noise by four times the standard deviation. If a seed is found all the neighboring cells which exceed the noise by at least two times the standard deviation are added to the cluster. Lastly all the cells neighboring these clusters are also added.

### 3.1.3 Matching Track to Cluster

The algorithm tries to match every track to one or more calorimeter clusters. First the algorithm tries to match a single best-match topo-cluster to every selected track. To do so first the distances in  $\Delta\phi$  and  $\Delta\eta$  from the track are extrapolated to the second layer of the EM calorimeter and then topo cluster. After that the topo-clusters get ranked based on the metric:

$$\Delta R' = \sqrt{\left(\frac{\Delta\phi}{\sigma_\phi}\right)^2 + \left(\frac{\Delta\eta}{\sigma_\eta}\right)^2} \quad (3.1)$$

where  $\sigma_\eta$  and  $\sigma_\phi$  refer to the angular topo-cluster width, computed from the standard deviation of the displacemtens of the topo clusters. If the energy in this cluster is greater or equal than the energy estimated from the track  $p_T$  the algorithm goes to cell subtraction. If not all clusters in a cone of  $\Delta R < 0.2$  are matched to the track. In that case R is calculated on the metric:

$$\Delta R = \sqrt{(\Delta\phi)^2 + (\Delta\eta)^2} \quad (3.2)$$

### 3.1.4 Cell Subtraction

The last step in the Particle Flow algorithm after matching a set of topo-clusters to a track is the cell-wise subtraction of energy deposits to remove remnants and determine which energy depositions belong to the given particle. If the energy deposited in the set of clusters falls below the expected energy the clusters are simply removed. Otherwise, a cell by cell subtraction is performed.

The first step of the cell subtraction is generating a shower shape from the extrapolated track. Around the extrapolated track rings in  $\eta, \phi$  space are generated, being just wide enough to independently contain

at least one one cell from the extrapolated position. Furthermore the rings are restricted to one layer and for each layer have the same radial size. After the generation of rings in each layer the average energy density in each ring is computed and the rings are ranked by energy density in descending order. The layer is not used in any way for this ranking. The subtraction then starts from the ring with highest energy density and proceeds successively to rings in lower order until the next ring's energy exceeds the remaining expected energy. If the ring's energy exceeds the energy still to be subtracted the energy in each cell is scaled down by the fraction needed to reach the expected energy then the process halts and the remaining cells are removed as remnants. An example of the process is sketched in figure 3.2.

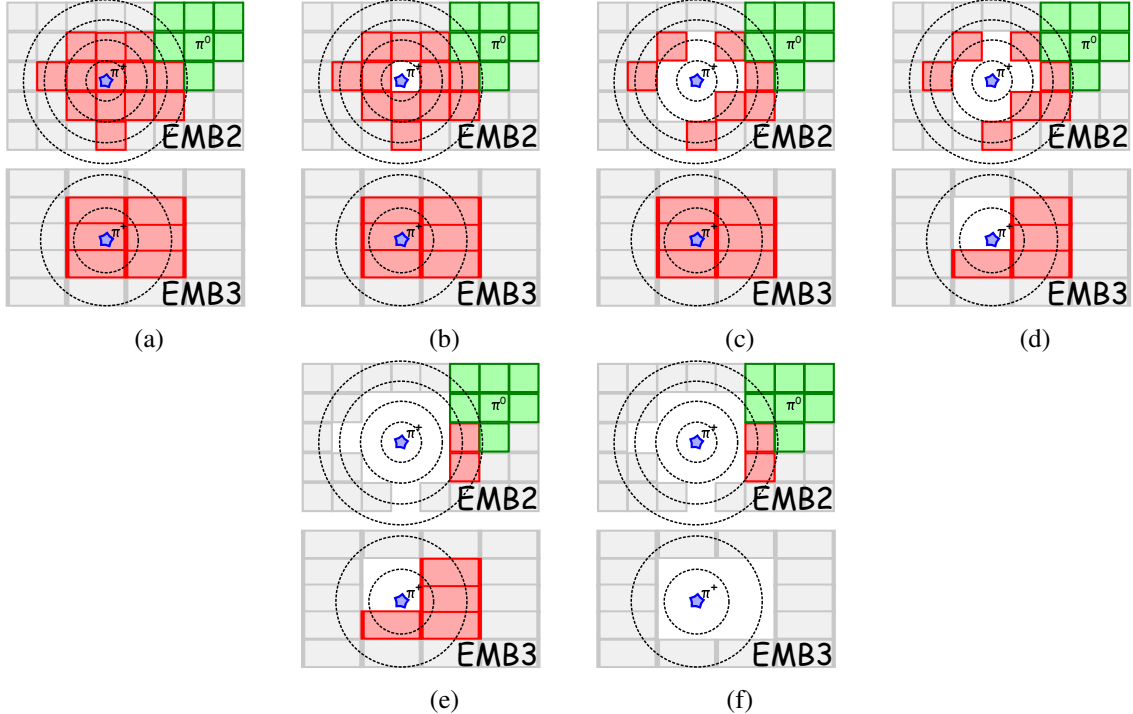


Figure 3.2: Example of cell subtraction. In red the depositions originating from the  $\pi^+$  of interest are shown and in green a cluster from a  $\pi^0$  are shown. [pflow16]

### 3.1.5 Eflow Rec performance studies

The Particle Flow paper shows the impact that the new algorithm had on the angular resolution and on the rejection of pileup jets. This section briefly summarizes the important results of the studies. Figure 3.3(a) and 3.3(b) show the improvements in angular resolution while figure 3.4 pictures the increased rejection of fake jets for the new algorithm. LC+JES jets are the jets using the old algorithm and JVJF in figure 3.4 refers to the Jet Vertex Fraction being the amount of energy in the jet originating from the original vertex.

The plots show clearly that Particle Flow improves the angular resolution in low  $p_T$  regions while having no drawback for higher  $p_T$  regions. The pileup contribution is also mediated massively even in comparison to the usage of a cut on the JVT. The region of effect is restricted to  $|\eta| < 2.5$  because only this region of pseudorapidity is covered by the Inner Detector. Only the momentum resolution shown in figure 3.5 becomes slightly worse than the resolution using the old reconstruction for high  $p_T$  regions.

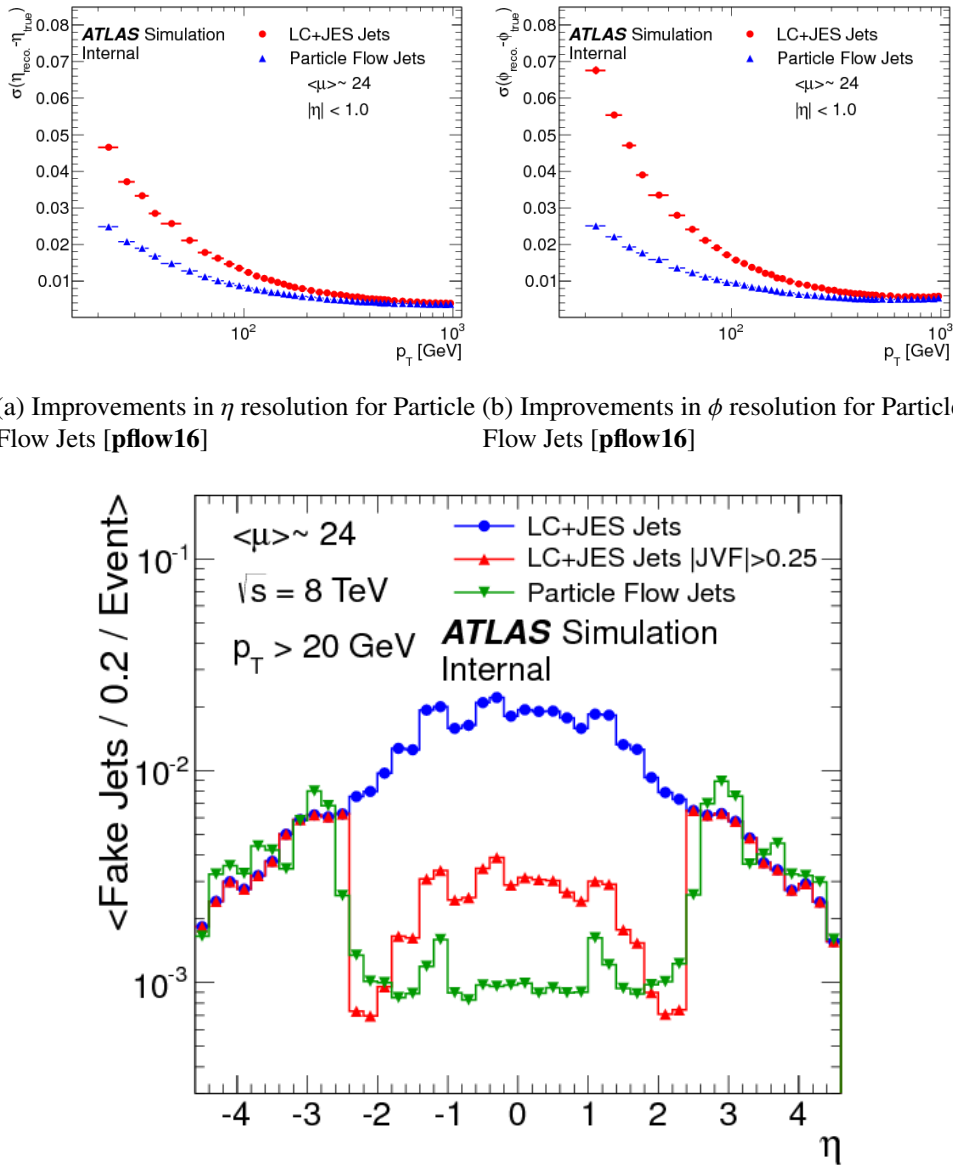


Figure 3.4: Pileup comparison of EM-Topo Jets and Particle Flow jets [pflow16]

### 3.1.6 Recent updates in eflowrec

The description of the Particle Flow algorithm given in this thesis is based on the analysis of Run 1 data and some recent changes to the algorithm are described in this section.

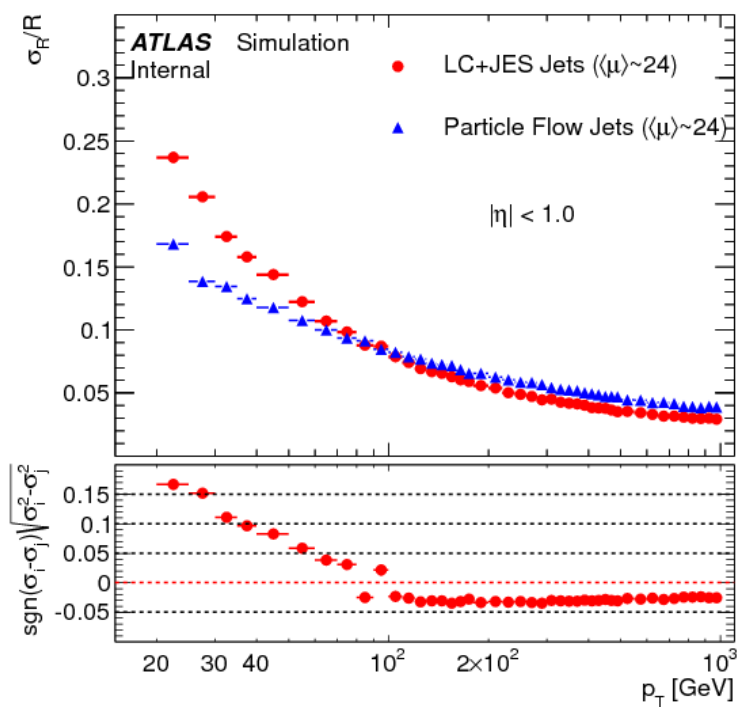


Figure 3.5: Momentum resolution of Particle Flow jets [pflow16]



# CHAPTER 4

---

## Analysis framework

---

To construct a framework for general Particle Flow analysis and data Monte Carlo comparison a large amount of ingredients is needed to be included and checked to be correctly working. In this chapter I will go over the important tools included in my framework. The impact of every given tool will be demonstrated and possible problems in current implementation are also included to summarize the status of the framework.

### 4.1 Jet cleaning

The Jet cleaning allows to apply certain requirements on jets in an event and therefore to remove jets or even complete events that might be bad data. The Jet Cleaning is used on both data and Monte Carlo to make sure that Monte Carlo events that would be removed in data also are not included in the simulation.

### 4.2 The Good Run List

The Good Run List is only needed for actual detector data. For data to be suitable for analysis one has to make sure that it fits certain requirements of which some depend on the detectors working state. The Good Run List allows to exclude data-taking periods in which the detector showed a poor working state. Reasons for this may be maintenance on sub detectors, magnets off or ramping or an unstable beam of the LHC. The Good Run List includes all the good data taking periods and the tool excludes all data from bad periods.

### 4.3 Jet Calibration and Smearing

After making sure a Jet is "good" and therefore has passed the cleaning it must still be calibrated and in case of MC smeared to data. The Calibration scales the energy of jets for a certain reconstruction algorithm. The Smearing smears the MC resolution to be matching the actual data resolution.

### 4.4 The jet vertex tagger

An important part of analysis is the rejection of pileup jets. A way to minimize pileup is to calculate the jet-vertex fraction of each jet which is the fraction of momentum in the jet originating from the primary

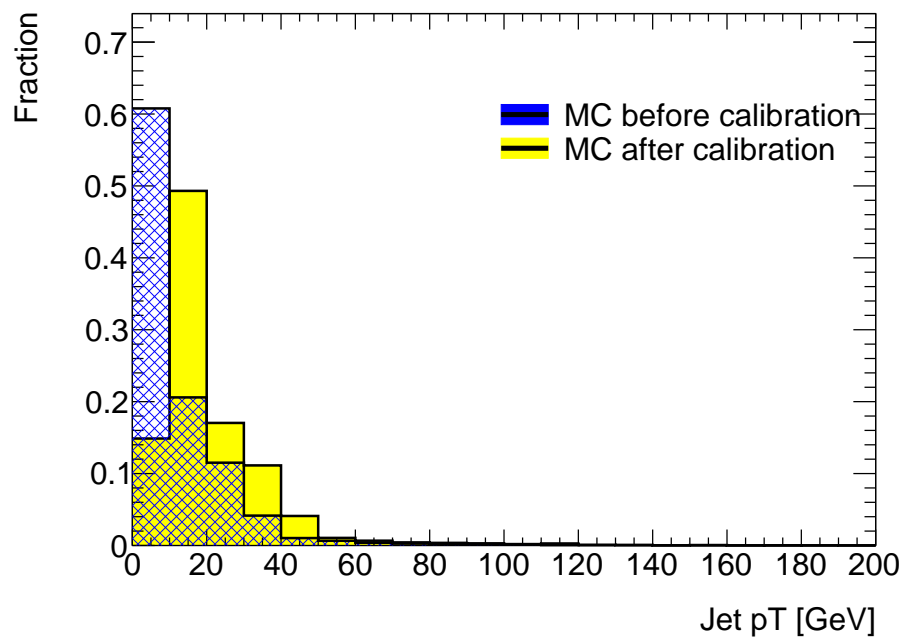


Figure 4.1: The influence of the calibration in momentum is shown

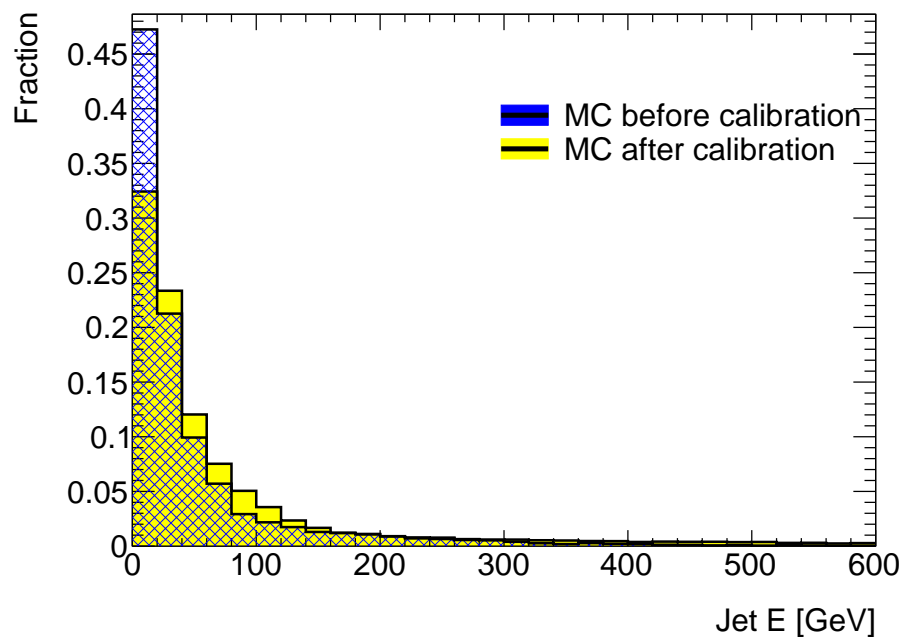


Figure 4.2: The influence of the calibration in energy is shown

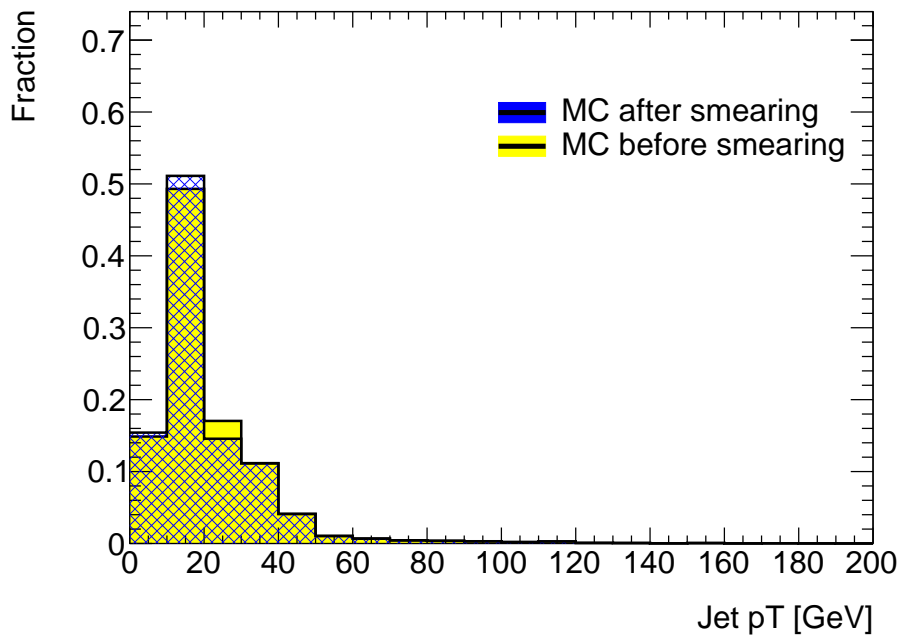


Figure 4.3: The influence of the Smearing in momentum is shown

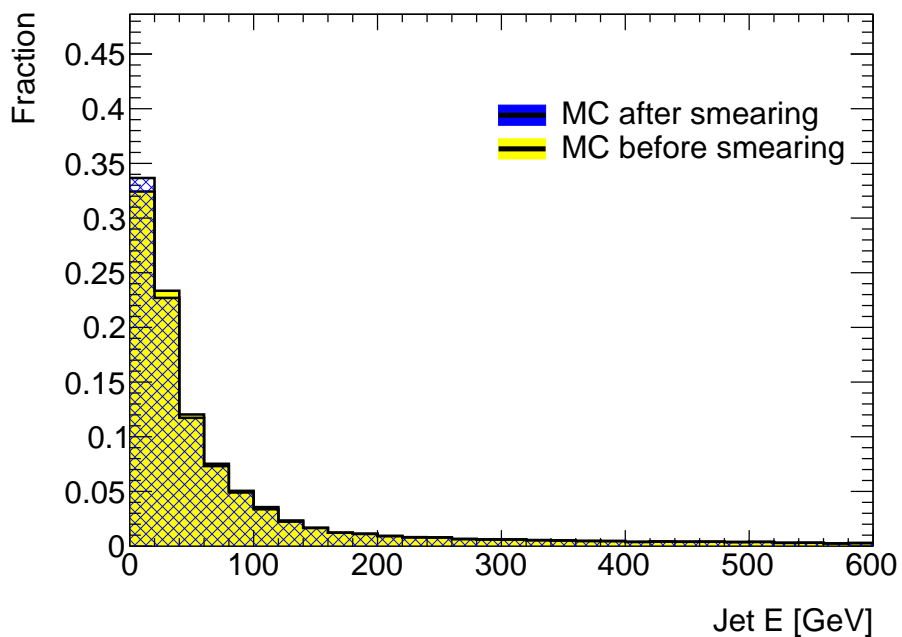


Figure 4.4: The influence of the Smearing in energy is shown

vertex. If one sets a minimum on this fraction pileup can be suppressed. The Jet Vertex Tagger related each jet to a vertex.

## **4.5 Trigger Tools**

A further important collection of tools has to make sure that the trigger is fired, correctly used and also that the particle that triggered is actually one of those used in later analysis.

A trigger basically is a first selection for an event meaning that an event is required to surpass certain demands to be used in analysis. These demands are embodied by so called trigger chains that can be used as input for a trigger tool in analysis which on that base can select or refuse events.

Usually the trigger is checked before the event is further cleaned and calibrated. Therefore it can happen that the particles that passed the trigger later get removed in the analysis. The trigger matching makes sure that the particles that passed the triggers are still left in the final analysis and if not the event can still be removed.

## **4.6 Monte Carlo Re-weighting**

The Monte Carlo is produced before data is taken therefore the shape of Monte Carlo may vary from the shape of the actual taken data for several reasons. For example the pileup in MC may not match the data as well as the resolution. To compensate these differences a sum of weights is applied to Monte Carlo.

## **4.7 Data Re-weighting**

## **4.8 Muon Calibration and Selection**

Analog to jets the muons in an event also have to go through several cuts and have to be calibrated properly. This section introduces all the important tools for muon calibration and gives a brief summary of the effects of the cuts and calibrations.

## **4.9 Electron Calibration and Selection**

The electron tools are the more or the less parallel to the muon tools and I will summarize and explain them in the same way.

# CHAPTER 5

---

## Results

---

### 5.1 The $Z \rightarrow \mu\mu$ decay

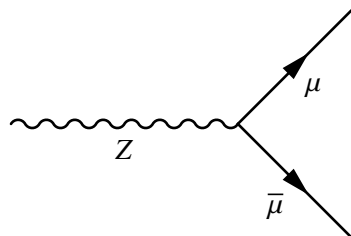


Figure 5.1: Decay of a Z-Boson to two muons

For this thesis  $Z \rightarrow \mu\mu$  events were used. The decay channel of a Z boson into a muon and an antimuon has a cross-section of  $3.366 \pm 0.007$  [pdg]. The event was chosen for this analysis because the Z boson is very easy to trigger on and it allows a very clear event selection. Furthermore the event has exactly one recoiling jet that analysis can be performed on.

### 5.2 Event Selection

The criteria for the event selection were no good electrons and exactly two good muons, with opposite charge where good means that the particle passed all selection filters itself. The reconstructed Z-Boson is required to be in a range of  $(90 \pm 10)$  GeV and to have a transversal momentum greater than 30 GeV while the muons are required to have a transversal momentum greater than 25 GeV. Furthermore the muons are restricted to a central  $\eta$  region being  $|\eta| < 2.4$ .

Furthermore a jet is required to have a transversal momentum greater than 20 GeV and is required to be recoiling to the reconstructed Z giving the selection criteria  $|\phi_{jet} - \phi_Z| < (\pi - 0.4)$ .

### 5.3 Results

I know nothing



## APPENDIX A

---

### Useful information

---

In the appendix you usually include extra information that should be documented in your thesis, but not interrupt the flow.



# List of Figures

---

2.1	Sketch of the LHC ring, the position of the experiments and the surrounding countryside.	5
2.2	Sketch of the ATLAS detector	6
2.3	Sketch of the transversal section of the ATLAS detector	7
3.1	Flowchart of the steps of the Particle Flow algorithm	10
3.2	Example of cell subtraction. In red the depositions originating from the $\pi^+$ of interest are shown and in green a cluster from a $\pi^0$ are shown. [pflow16]	11
3.4	Pileup comparison of EM-Topo Jets and Particle Flow jets	12
3.5	Momentum resolution of Particle Flow	13
4.1	Influence of the JES on the transversal momentum	16
4.2	Influence of the JES on the energy	16
4.3	Influence of the Smearing on the transversal momentum	17
4.4	Influence of the Smearing on the energy	17
5.1	Decay of a Z-Boson to two muons	19



# List of Tables

---

2.1	Lepton properties	4
2.2	Quark properties	4
2.3	Mediator properties	4